Central European Geology, Vol. 52/1, pp. 51–72 (2009)
DOI: 10.1556/CEuGeol.52.2009.1.4

Bimodal pumice populations in the 13.5 Ma Harsány ignimbrite, Bükkalja Volcanic Field, Northern Hungary: Syn-eruptive mingling of distinct rhyolitic magma batches?

Réka Lukács, Szabolcs Harangi,
Department of Petrology and Geochemistry
Eötvös Loránd University, Budapest

Paul R. D. Mason
Vening Meinesz Research School of Geodynamics
Department of Earth Sciences, Utrecht University
Utrecht

Theodoros Ntaflos
Institute of Lithosphere Studies,
University of Vienna, Vienna

The 13.5 Ma Harsány ignimbrite, in the eastern part of the Bükkalja volcanic field, eastern-central Europe, provides a rare example of mingled rhyolite. It consists of two distinct pumice populations ('A'- and 'B'-type) that can be recognized only by detailed geochemical work. The pumice and the host ignimbrite have a similar mineral assemblage involving quartz, plagioclase, biotite and sporadic K-feldspar. Zircon, allanite, apatite and ilmenite occur as accessory minerals. The distinct pumice types are recognized by their different trace element compositions and the different CaO contents of their groundmass glasses. Plagioclase has an overlapping composition; however, biotite shows bimodal composition. Based on trace element and major element modeling, a derivation of 'A'-type rhyolite magma from the 'B'-type magma by fractional crystallization is excluded. Thus, the two pumice types represent two isolated rhyolite magma batches, possibly residing in the same crystal mush. Coeval remobilization of the felsic magmas might be initiated by intrusion of hot basaltic magma into the silicic magma reservoir The rapid ascent of the foaming rhyolite magmas enabled only a short-lived interaction and thus, a syn-eruptive mingling between the two magma batches.

Key words: mingling, pumice, rhyolite, ignimbrite, Bükkalja volcanic field, Pannonian Basin

Introduction

Rhyolitic ignimbrite and associated ash fall deposits are the products of voluminous volcanic eruptions (Bachmann et al. 2002; Hildreth 2004; Wilson et al. 2006; Hildreth and Wilson 2007). Some of these eruptions result in compositionally homogeneous varieties; others provide compositionally zoned

Addresses: R. Lukács, Sz. Harangi: H-1117 Budapest, Pázmány Péter sétány 1/C, Hungary,
e-mail: lrekuska@freemail.hu
P. R. D. Mason: Budapestlaan 4, 3584 CD Utrecht, The Netherlands
T. Ntaflos: Althanstrasse 14, A-1090 Vienna, Austria
Received: June 8 2009; accepted: June 30, 2009

deposits with crystal-poor and crystal-rich ones. These features reflect the processes occurring prior to violent eruptions. Beneath the rhyolitic volcanic provinces extensive magma reservoirs develop, often several kilometers thick and several kilometers (sometimes several tens of kilometers) wide. Understanding the behavior of such huge and long-lived magmatic systems is crucial for the evaluation of the nature of large-volume volcanic eruptions and to obtaining an insight into deep crustal processes. Recent works emphasize the mush model of silicic magmatism (Bachmann and Bergantz 2004, 2008; Hildreth 2004; Hildreth and Wilson 2007), meaning that eruptible high-silicic magma types are accumulated incrementally at the roof zone of a huge crystal-rich mush. During the 10^5-yr scale life-time of such systems, several melt batches intrude into the magma reservoir, resulting in sequential growing of the rhyolite magmas and the silicic plutons (Wark et al. 2007). In addition, several cycles of crystallization and melting take place, often accompanied by pre-eruptive convective mixing and syn-eruptive disruption of distinct zones in the pre-eruption magma body (Bachmann et al. 2007). The reconstruction of these complex processes can be achieved by detailed textural and geochemical investigation of the mineral phases and the glass content of the pumice and fine-grained ash fraction.

During the formation of the Pannonian Basin, extensive silicic volcanic eruptions occurred from 20 Ma to 13 Ma, often producing several 100 meter-thick pyroclastic deposits, usually ignimbrite sheets (Póka 1988; Szabó et al. 1992; Márton and Pécskay 1998; Harangi 2001; Pécskay et al. 2006; Harangi and Lenkey 2007). This could also have had a major impact in the crustal evolution. Although most of these volcanic products are buried by younger sediments, they can be excellently studied in the foreland of the Bükk Mts. (Bükkalja Volcanic Field). Within the ignimbrite sequence, both homogeneous crystal-poor and heterogeneous crystal-rich varieties were formed (Szakács et al. 1998; Harangi et al. 2005). In addition, there are many examples of the occurrence of distinct juvenile clasts in single pyroclastic flow units, an indication of magma mixing or mingling (Póka et al. 1998; Czuppon et al. 2001; Lukács and Harangi 2002; Harangi et al. 2002; Lukács et al. 2007). Recently, Lukács et al. (2007) described the 13.5 Ma Harsány ignimbrite, where two rhyolitic pumice populations were recognized. It is noteworthy that the bimodal pumice character of this ignimbrite cannot be recognized in the field, but only by detailed geochemical work. Based on the geochemical data of the pumice, the glass and the mineral phases, this paper provides an insight into the nature of the silicic magmatic system. It shows an example of mingling of two rhyolitic magmas derived from spatially separated magma batches.

Geologic background

The Harsány ignimbrite unit (Lukács et al. 2007) is the youngest member of the silicic pyroclastic succession of the Bükkalja Volcanic Field (BVF; Fig. 1). The BVF exposes the products of the extensive Miocene silicic volcanic activities in the Pannonian Basin (Póka et al. 1988; Szakács et al. 1998; Lukács et al. 2001, 2005; Harangi et al. 2005; Márton et al. 2007). These volcanic rocks were formed between 21 Ma and 13.5 Ma (Márton and Pécskay 1998) and consist only of

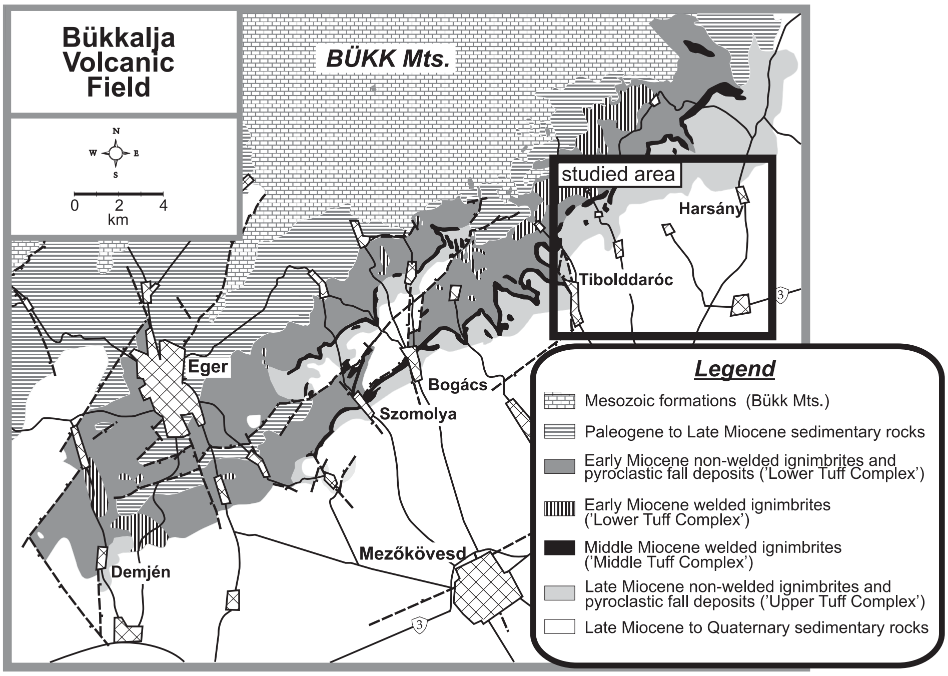

Fig. 1
Simplified geologic map of the Bükkalja Volcanic Field (after Szakács et al. 1998 and Harangi et al. 2005) with the studied area

pyroclastic rocks. They are mostly non-welded to welded pumice-rich pyroclastic flow deposits (ignimbrite); scoria-bearing pyroclastic flow, pyroclastic fall and phreatomagmatic fall deposits occur subordinately (Pantó 1962; Capaccioni et al. 1995; Szakács et al. 1998; Harangi et al. 2005). The volcanic succession has been successfully divided into three main units based on paleomagnetic data (Lower, Middle, Upper Tuff Complexes; Márton and Pécskay 1998; Márton et al. 2007), because two major rotation events occurred in this area during the Miocene (Márton and Fodor 1995). However, geochemistry-based correlation studies pointed out that there are distinct ignimbrite units even between two rotation events (Póka et al. 1998; Lukács et al. 2001, 2007; Harangi et al. 2005).

The juvenile fragments are dacite to rhyolite pumice and basaltic andesite to andesite scoria, whereas the associated cognate lithic clasts have compositions from basaltic andesite to rhyolite (Harangi 2001). The composition of juvenile clasts shows a mainly calc-alkaline geochemical character; however, the origin of these rocks is still a subject of debate. Crustal anatexis for the magmas of the Lower and Upper Tuff Complexes was suggested by Lexa and Konecný (1998) and Póka et al. (1998), whereas Harangi (2001), Seghedi et al. (2004) and Harangi et al. (2005) emphasized the role of mantle-derived mafic magmas in the origin of the BVF silicic volcanic rocks. In addition, magma mixing could also have been important, especially in the genesis of the dacitic-rhyolitic rocks of the Middle Tuff Complex (Póka et al. 1998; Czuppon et al. 2001; Harangi et al. 2002, 2005).

The Harsány ignimbrite unit

The Harsány ignimbrite unit (Lukács et al. 2007) crops out in the eastern part of the BVF (Fig. 1) around the villages of Harsány and Tibolddaróc, but it continues further eastward in the subsurface (Lukács et al., in press). It is an unsorted, pumice-rich pyroclastic flow deposit, which overlays the pyroclastic succession of the Middle Tuff Complex. It is at least 15 meters thick and contains large amounts of lapilli- and block-sized rhyolitic pumice clasts (Fig. 2). The size of the pumice clasts can reach 40 centimeters; they do not differ macroscopically

Fig. 2
Typical appearance of the Harsány ignimbrite. The size of the largest pumice (bottom right) is 28 cm

from each other. The strongly vesiculated texture of the pumice and the cuspate-shaped glass shards indicate magmatic explosive fragmentation. In addition to the juvenile components (30–40 vol%), lithic clasts can also be found in 1–5 vol% amounts; they are mainly rhyolitic obsidian and minor amounts of metamorphic fragments from the basement. The common presence of obsidian lithic fragments could indicate intra-caldera rhyolitic lava flows just prior to the plinian explosive eruption. The K/Ar radiometric age dating on separated biotite fractions from two localities of the ignimbrite yielded 13.5 Ma (Lukács et al. 2007).

The phenocryst assemblage of the ignimbrite includes quartz (30%), plagioclase (55%), biotite (10%) and sporadic K-feldspar (<5%). The pumice is phenocryst-poor (<10 vol%) and has the same mineral assemblage as the host ignimbrite. Macroscopically the large (max. 6 millimeters) quartz crystals have a typical pale violet color in the pumice. Silicate melt inclusions of variable texture can often be observed in quartz and plagioclase (Lukács et al. 2002). The accessory mineral assemblage consists of zircon, allanite, apatite and ilmenite. The zircon morphology shows a bimodal population (Szabó 2000; Szabó and Harangi 2001). One of the zircon groups is of a typical hybrid calc-alkaline character with dominant S_8 and S_{13} morphology, whereas the other shows mantle-derived alkaline character with $P_{2–3}$ morphology.

Sampling and analytical methods

Bulk ignimbrite and single pumice samples for petrologic and geochemical analyses were collected from two localities (northern end of Harsány village and at the wine cellar district of Tibolddaróc). When sampling the pumice we took great care to select fresh samples and to randomly collect samples of different sizes from the outcrops. Beside the juvenile pumice samples we also collected several lithic clasts from the ignimbrite.

The major and trace elements of the single pumice clasts and the lithic clasts were determined by XRF spectrometry, ICP-AES and INAA. The XRF analyses were carried out at the Department of Lithospheric Studies of the University of Vienna (Austria) using a PHILIPS PW2400 sequential X-ray spectrometer with a super-sharp end-window tube and a Rh anode and a 3 kW generator. The rare earth elements were measured by ICP-AES at the Royal Holloway College, Egham (UK) using the method of Walsh et al. (1981) and by INAA at the Institute of Nuclear Techniques, Technical University of Budapest (Hungary). During the INAA measurements, we used 2.4*1012 $ncm^{-2}s^{-1}$ thermal neutron flux for 8 hours, and the measurements were carried out with a Canberra HPGE Well-type detector and a Canberra S100 multichannel analyzer. For the evaluation of spectra, SAMPO 90 software was used. Standardization was carried out with the single comparator method (DeCorte 1987) using Au as the comparator element. The results of the ICP-AES and INAA were checked by using a common sample for both analyses. We obtained the same values within the analytical errors.

$^{87}Sr/^{86}Sr$ and $^{143}Nd/^{144}Nd$ isotope ratios of two pumice samples were determined by VG354 multicollector mass-spectrometer as described in Harangi et al. (2007).

The major elements of the juvenile glass and phenocrysts were analyzed with a CAMECA SX100 electron microprobe using 15 kV voltage and 20 nA beam current at the Institute of Earth Sciences, University of Vienna (Austria). For the glass we used a defocused beam to minimize the alkali loss. The trace element analyses were performed with a LA-ICP-MS using a 193 nm ArF excimer laser ablation system (MicroLas GeoLas 200Q) in combination with an ICP-MS (Micromass Platform ICP) at Utrecht University (Netherlands) (Mason and Kraan 2002). Details of the measurements can be found in Harangi et al. (2005).

Bulk rock geochemistry

We analyzed randomly selected single pumice samples and rhyolitic lithic clasts from two localities of the Harsány ignimbrite unit. The major and trace element compositions are presented in Table 1. The pumice and lithic clasts show fairly similar major element compositions: they are high-silica potassic rhyolite of slightly peraluminous character (SiO_2=74.7–77.2 wt%, K_2O=3.6-5.3 wt%, K_2O/Na_2O= 1.1–2.2; Fig. 3). However, slight differences can be observed between the pumice clasts in CaO and K_2O contents that are also corroborated by the different trace element contents.

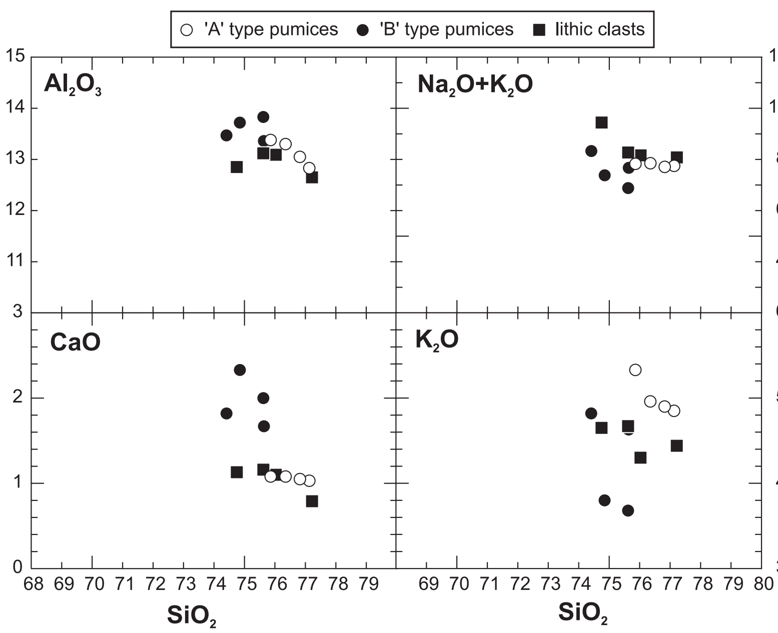

Fig. 3
Major element characteristics of the pumice clasts and lithic clasts from the Harsány ignimbrite

Table 1
Major element (in wt%) and trace element (in ppm) composition of pumice and lithic clasts of the Harsány ignimbrite. Major elements are recalculated to 100%, anhydrous base. n.d.: non-determined

Sample	**N22**	**H-1**	**H2-2P3**	**H1-1**	**H1-2**	**BK41-L3**	**H1-L1**	**H5-1**	**H5-2**	**T-1**	**TD16P1**	**N9**
Locality	**Harsány**	**Harsány**	**Harsány**	**Harsány**	**Harsány**	**Harsány**	**Harsány**	**Harsány**	**Harsány**	**Tibold-daróc**	**Tibold-daróc**	**Tibold-daróc**
Type	**'A'-type pumice**	**'B'-type pumice**	**'B'-type pumice**	**'A'-type pumice**	**'A'-type pumice**	**lithic clast**	**lithic clast**	**lithic clast**	**lithic clast**	**'A'-type pumice**	**'B'-type pumice**	**'B'-type pumice**
SiO_2	76.35	75.62	78.21	77.13	76.82	77.22	74.75	76.03	75.62	75.86	74.85	75.64
TiO_2	0.10	0.27	0.16	0.09	0.10	0.07	0.13	0.13	0.14	0.11	0.26	0.19
Al_2O_3	13.30	13.83	12.04	12.83	13.05	12.65	12.85	13.09	13.12	13.38	13.72	13.36
Fe_2O_3	1.13	1.16	1.64	0.97	1.04	0.99	1.42	1.23	1.36	1.49	1.17	1.26
MnO	0.04	0.02	0.04	0.03	0.04	0.04	0.04	0.02	0.05	0.05	0.03	0.03
MgO	0.13	0.13	0.29	0.14	0.17	0.12	0.20	0.19	0.24	0.17	0.18	0.14
CaO	1.08	2.00	1.87	1.03	1.05	0.79	1.13	1.10	1.16	1.08	2.33	1.67
Na_2O	2.89	3.20	2.11	2.90	2.81	3.64	4.79	3.86	3.60	2.50	3.58	3.04
K_2O	4.96	3.68	3.65	4.85	4.90	4.44	4.65	4.30	4.67	5.33	3.80	4.63
P_2O_5	0.03	0.07	0	0.03	0.03	0.03	0.04	0.04	0.04	0.03	0.07	0.04
LOI	2.39	3.39	3.7	3.63	3.56	2.39	0.24	0.70	2.77	4.12	3.54	2.93
Ni	4	9.2	1.3	n.d.	n.d.	n.d.	n.d.	n.d.	n.d.	12.7	n.d.	3
Cr	4	n.d.	n.d.	n.d.	n.d.	n.d.	n.d.	n.d.	n.d.	n.d.	7	6
Sc	4.68	4.2	4	4.42		4	5.1		3.5	5.1	3.5	5.8
Co	44.6	1.06	1.7	0.74	2.2	0.61	0.87	2.5	2.6	1.18	0.99	n.d.
Rb	153	86.3	119.9	133.7	132.9	147.9	138.5	131.5	132.8	161	69.5	110
Ba	836	1013.2	714	819.1	919.1	666.6	730.1	858.3	866.7	885.7	825.3	976
Pb	18.1	14.8	0.8	n.d.	n.d.	n.d.	n.d.	n.d.	n.d.	16.2	n.d.	16.9
Sr	73	144.1	137.5	65.7	69.1	41.6	65.3	73.8	73.7	65.6	175	126
Zr	108	209.9	99	82.2	85.9	79.9	128.6	105.1	103.8	91.2	188.7	161
Nb	14	13	11.6	9.3	8.8	9.6	12.5	9.7	10	10.8	9.7	14
Y	35	20.6	14.9	28.8	28.1	34.3	34.8	30.3	30.1	32.1	16.3	24
Th	12.9	12.6	14.4	12.4	n.d.	14.6	14.6	n.d.	n.d.	13.1	10.2	13.8
La	28.5	64.9	35.6	23	17.6	22.1	32.4	23.5	27.2	26.8	50.9	49.21
Ce	58.91	110	61.4	45	45.7	45	62	54.3	60.7	54	89	93.73
Nd	22.7	32	20.5	16	n.d.	15	20	n.d.	n.d.	18	29	29.9
Sm	4.68	4.84	3.1	4.01	n.d.	4.31	5.48	n.d.	n.d.	4.38	4.04	4.82
Eu	0.59	0.98	0.6	0.47	n.d.	0.36	0.66	n.d.	n.d.	0.62	0.96	0.86
Gd	4.84	n.d.	2.37	n.d.	n.d.	n.d.	n.d.	n.d.	n.d.	n.d.	n.d.	4.21
Dy	5.15	n.d.	2.44	n.d.	n.d.	n.d.	n.d.	n.d.	n.d.	n.d.	n.d.	3.73
Ho	1.05	n.d.	0.46	n.d.	n.d.	n.d.	n.d.	n.d.	n.d.	n.d.	n.d.	0.75
Er	2.74	n.d.	1.45	n.d.	n.d.	n.d.	n.d.	n.d.	n.d.	n.d.	n.d.	1.81
Yb	3.18	1.96	1.63	3.14	n.d.	3.93	4.07	n.d.	n.d.	3.19	1.75	2.15
Lu	0.51	0.3	0.26	0.44	n.d.	0.55	0.56	n.d.	n.d.	0.47	0.29	0.36
Cs	5.01	2.77	4.5	4.74	n.d.	5.91	3.04	n.d.	n.d.	4.76	2.12	n.d.
Hf	3.46	5.41	3.2	3.3	n.d.	3.19	5.04	n.d.	n.d.	3.51	5.13	n.d.
Ta	1.69	1.04	1	1.27	n.d.	1.47	1.55	n.d.	n.d.	1.29	0.9	n.d.
U	4.5	3.1	5.4	4.3	n.d.	5.6	3.8	n.d.	n.d.	4	2.9	n.d.

Table 2
Sr and Nd isotope data for the two pumice types of the Harsány ignimbrite. The initial Sr-isotope ratios were calculated using a 13.5 Ma age

Sample	Locality	Type	$^{87}Sr/^{86}Sr$	$^{87}Sr/^{86}Sr_o$	$^{143}Nd/^{144}Nd$
N9	Tibolddaróc	'B'-type pumice	0.70799	0.70734	0.51245
N22	Harsány	'A'-type pumice	0.70943	0.70787	0.51244

The pumice samples can be divided into two groups based on their trace element characteristics, denoted here as 'A'-type and 'B'-type pumice groups. The two pumice types are randomly distributed in the ignimbrites and are each represented here by four samples. In addition, four rhyolitic lithoclasts show 'A'-type pumice composition (Fig. 3). The two pumice groups differ from one another in their REE patterns and their Rb, Sr, Y, P and Ti contents. The 'B'-type pumice has a smaller negative Eu-anomaly (Eu/Eu*=0.57), higher light REE and lower heavy REE contents than the 'A'-type one (Eu/Eu*=0.38). In general, all the samples have "subduction-related" trace element pattern, with relative LILE enrichment, a negative Nb, Sr, Ti, P, and a positive Pb anomaly.

Two pumice samples, one of each type, were analyzed for $^{143}Nd/^{144}Nd$ and $^{87}Sr/^{86}Sr$ isotope ratios (Table 2). They have the same initial $^{143}Nd/^{144}Nd$ isotope ratio ($^{143}Nd/^{144}Nd$=0.51245) and only slightly different initial $^{87}Sr/^{86}Sr$ value (0.7073 and 0.7079, respectively). It is remarkable that these isotope ratios are different from those of the pumices of the Lower and Middle Tuff Complexes of the BVF ($^{143}Nd/^{144}Nd$=0.51220–0.51225 and $^{87}Sr/^{86}Sro$=0.7100–0.7120; Harangi 2001), but are within the Sr–Nd isotope range of the Badenian (16–14 Ma) calc-alkaline andesite of the Northern Pannonian Basin ($^{143}Nd/^{144}Nd$=0.51235–0.51250 and $^{87}Sr/^{86}Sro$=0.7065–0.7085; Harangi et al. 2007).

Glass chemistry

Glass shards of the bulk ignimbrites and the glassy groundmass of the pumice blocks are remarkably fresh and their compositions show a high silica (SiO_2=77.08–79.18 wt%) and high potassium (K_2O=3.75–6.18 wt%) character. Representative compositions are presented in Table 3. Their calculated water-content (based on the division method; Devine et al. 1995; Blundy and Cashman 2001) is mostly within the range of 4 and 6.5 wt%, what is consistent with the usual water content of rhyolitic magma (3–7 wt%; Lowenstern 1995). A smaller group has only 1.5–3 wt% water. Major element concentrations of the glass shards are very similar; however, the CaO content reflects two groups (Fig. 4). One of these has lower CaO values (0.54–0.67 wt%), characterizing most of the glass shards in the bulk ignimbrite as well as the glassy groundmass of the 'A'-type pumices. The glassy groundmass of the 'B'-type pumice typically has a

Table 3
Major element (in wt%) and trace element (in ppm) composition of glass shards and pumice glass of the Harsány ignimbrite. Major elements are recalculated to 100%, anhydrous base. LOI* is estimated based on the division method (Devine et al. 1995); n.d.: non-determined

Locality	Harsány				Tibolddaróc						Harsány		Tibolddaróc		
Sample	N20-2-1	N20-1-1	N20-5-2	N20-4-2	TD2-6-2	TD2-7	TD2-9	TD2-10	TD2-11	TD2-15	N20-17	N20-18	N9_02	N9_05	N9_06
Type	A'	A'	A'	A'	A'	A'	A'	A'	A'	A'	B'	B'	B'	B'	B'
SiO_2	77.33	77.66	78.15	78.29	77.86	77.56	77.38	77.62	77.73	77.81	78.38	78.73	78.19	78.38	78.81
TiO_2	n.d.	0.06	n.d.	n.d.	n.d.	n.d.	0.06	n.d.	0.04	0.03	0.09	0.10	0.05	0.08	0.06
Al_2O_3	13.25	12.89	12.87	12.89	12.90	12.93	12.89	12.97	12.89	12.61	13.08	12.82	13.09	12.83	12.86
FeO*	0.71	0.52	0.40	0.26	0.81	0.84	0.89	0.86	0.84	0.81	0.73	0.75	0.98	0.99	1.00
MnO	0.06	n.d.	n.d.	n.d.	0.07	0.07	0.05	0.05	0.05	0.06	0.05	0.04	0.04	0.04	0.04
MgO	0.07	n.d.	n.d.	n.d.	n.d.	n.d.	0.04	0.04	n.d.	n.d.	0.07	0.07	0.07	0.07	0.08
CaO	0.62	0.61	0.59	0.61	0.60	0.60	0.57	0.62	0.61	0.60	0.88	0.87	0.83	0.84	0.84
Na_2O	3.38	3.38	2.73	2.16	2.28	2.46	2.06	2.74	2.16	2.22	2.45	2.31	1.98	1.94	2.41
K_2O	4.58	4.87	5.16	5.71	5.44	5.47	6.06	5.10	5.64	5.83	4.27	4.31	4.77	4.82	3.90
LOI*	4.60	4.50	5.09	4.95	5.03	4.79	4.99	4.88	5.20	4.26	5.19	5.55	5.89	5.45	6.09
Rb	139	137	156	161	176	144	153	162	190	163	101	111	95	96	88
Ba	614	568	568	588	604	536	620	565	648	559	795	709	742	761	720
Sr	30.8	29.3	28.1	27.2	28.8	34.0	26.4	31.0	31.0	31.1	42.9	39.2	39.6	39.8	39.6
Y	27.1	26.6	32.0	25.3	32.9	26.2	34.0	28.8	36.8	30.2	17.0	14.6	17.7	17.3	16.2
Zr	55.8	51.3	52.8	47.4	79.0	68.5	56.7	56.9	68.6	63.9	51.1	49.4	56.1	53.2	53.8
Nb	9.90	10.10	11.64	10.70	14.40	9.49	12.00	12.40	13.96	11.24	9.26	8.11	9.68	9.04	8.48
La	17.20	15.40	15.24	16.10	19.41	20.61	18.50	18.10	19.64	17.35	28.34	25.03	26.24	27.68	26.56
Ce	32.80	30.50	32.76	35.70	42.21	36.98	39.50	37.70	39.71	35.78	55.54	49.26	48.16	52.16	50.48
Pr	4.10	3.50	4.08	3.60	4.59	4.04	4.20	4.10	4.91	4.04	5.14	4.91	5.04	5.68	5.28
Nd	14.30	14.70	16.20	15.00	19.09	14.61	16.60	14.40	18.33	15.16	19.66	17.94	17.20	18.64	17.20
Sm	3.80	3.30	3.78	3.80	4.41	3.39	4.15	3.65	4.47	3.76	3.03	3.14	3.24	3.24	3.20
Eu	0.32	0.38	0.33	0.46	0.28	0.35	0.29	0.32	0.31	0.29	0.57	0.39	0.46	0.50	0.49
Gd	4.70	3.40	4.56	3.60	4.36	4.36	5.10	4.00	4.47	3.60	3.66	2.29	3.10	3.82	2.84
Dy	4.80	4.80	5.04	4.50	5.56	4.91	5.10	4.80	5.89	4.69	1.89	2.57	3.48	3.60	3.40
Er	2.95	2.75	3.42	2.55	3.27	2.79	3.40	3.00	3.16	2.89	1.49	1.26	1.68	2.00	2.00
Yb	3.00	3.00	3.36	3.10	3.55	2.84	3.50	2.95	3.81	3.33	1.83	1.43	2.36	2.08	1.80
Lu	0.42	0.34	0.45	0.28	0.55	0.33	0.52	0.48	0.45	0.56	0.21	0.18	0.30	0.32	0.38
Hf	2.20	2.30	2.88	2.30	2.51	2.07	2.80	2.30	2.51	2.51	1.94	1.60	2.00	2.08	1.92
Ta	1.09	1.12	1.19	1.10	1.31	1.09	1.40	1.20	1.41	1.31	1.03	0.80	n.d.	n.d.	n.d.
Pb	18.60	19.00	20.40	22.90	22.15	18.21	21.00	19.90	25.53	19.64	23.31	25.60	13.12	14.16	12.88
Th	11.30	10.70	12.12	11.20	13.20	9.93	13.20	11.80	13.20	11.45	10.17	8.57	9.44	9.52	9.52
U	3.60	3.50	4.56	5.10	4.47	3.27	4.90	4.40	4.59	3.60	2.51	2.51	2.40	2.64	2.48

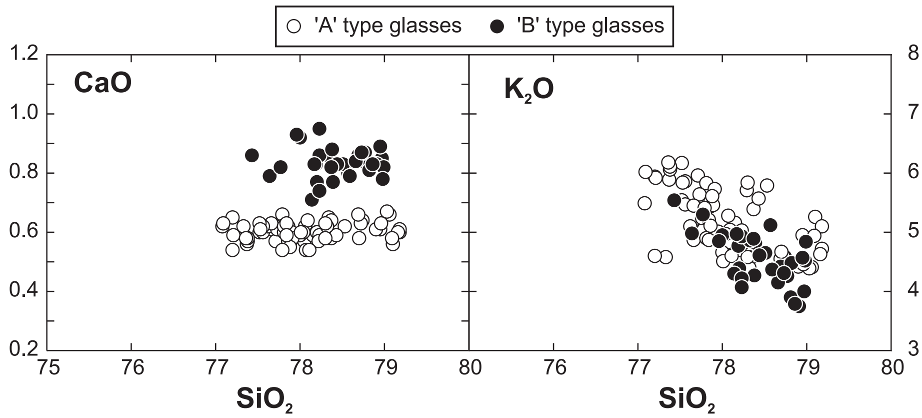

Fig. 4
Major element characteristics of the glass shards from the Harsány ignimbrite. Note the difference between the 'A'-type and 'B'-type glass in terms of Ca content

higher CaO content (0.71–0.95 wt%). Remarkably, only a few pumiceous glass shards have such composition in the bulk ignimbrite.

The trace element composition of the glass provides a more obvious distinction between the two pumice types. The 'B'-type glass differs significantly from the 'A'-type glass based on its La, Ce, Y, Yb, Nb, Rb, Ba, Sr, Th and U contents (Fig. 5). The negative Eu anomaly of the 'B'-type glass is typically smaller (Eu/Eu*=0.35–0.52) than that of the 'A'-type glass (Eu/Eu*=0.12–0.38). It is important to note that there are no transitional types between the two glass groups. The difference in the trace element content of the glass types is also reflected by the trace element composition of the two pumice groups (Fig. 5).

Mineral compositions

Feldspar is the most abundant mineral in the Harsány ignimbrite and the pumice blocks. Its composition is largely homogeneous (Lukács et al. 2007), although normal and oscillatory zoning can be occasionally found. The composition of the plagioclase shows a variation from sodic labradorite to oligoclase (An=52.8–16.6 mol%; Fig. 6). Sanidine (Or=65–70 mol%) occurs subordinately, but never in the 'B'-type pumice. Plagioclase in the 'B'-type pumice clasts has a more restricted composition (An=20–35 mol%), except for a single crystal core analysis (An=52.8 mol%), than those found in the 'A'-type pumice and in the bulk ignimbrite (An=16.6–50.2 mol%), but most of the data overlap each other.

Biotite is the only ferromagnesian phase in the Harsány ignimbrite. It is altered in various degrees and only a few grains appear to have their original composition (Table 4). In the BVF, biotite chemistry is a useful discriminator

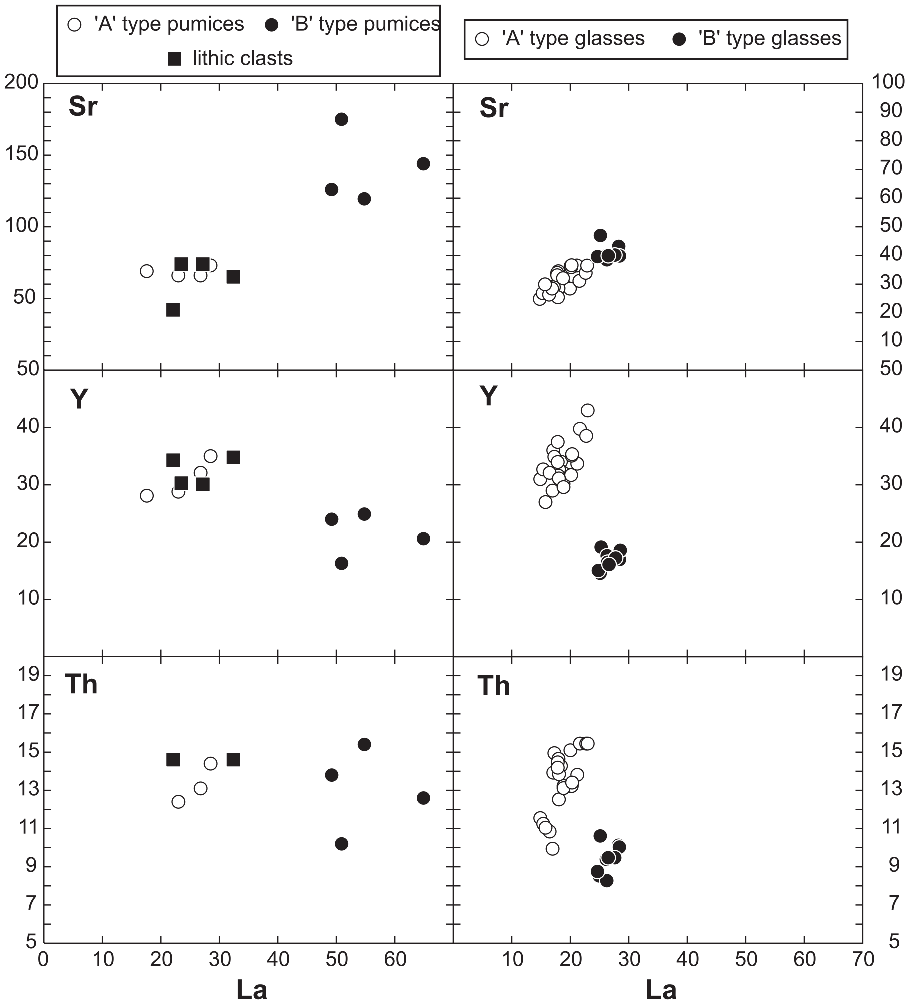

Fig. 5
Trace element characteristics of the pumice and lithic clasts and the glass shards from the Harsány ignimbrite. The two types of pumice and glass can clearly be separated

between the different ignimbrite units (Harangi et al. 2005). In the Harsány ignimbrite unit biotite shows a strong bimodal composition and this bimodality is consistent with the pumice types. The majority of the biotite data shows a relatively high iron (FeO=28–29 wt%, mg-number=0.24–0.28), and low TiO_2 contents (TiO_2=3.5–4 wt%; Fig. 7). It belongs to the 'A'-type pumice or is found in the bulk ignimbrite. The biotite in the 'B'-type pumices has significantly lower iron (FeO=22.8–23.6 wt%, mg-number=0.39–0.41) and higher titanium contents (TiO_2=4.5–5.1 wt%). The Al_2O_3 content of biotite shows a more restricted range between 12.8 and 13.7 wt% and no distinction between the pumice types.

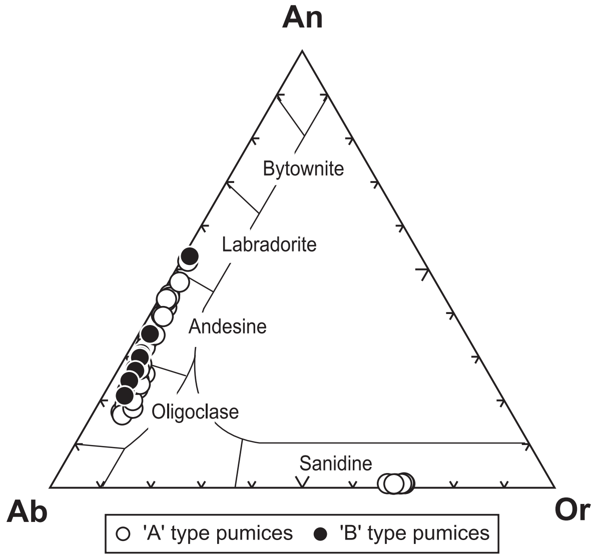

Fig. 6
Feldspar classification in the Ab-An-Or diagram. Data are from Lukács et al. (2007)

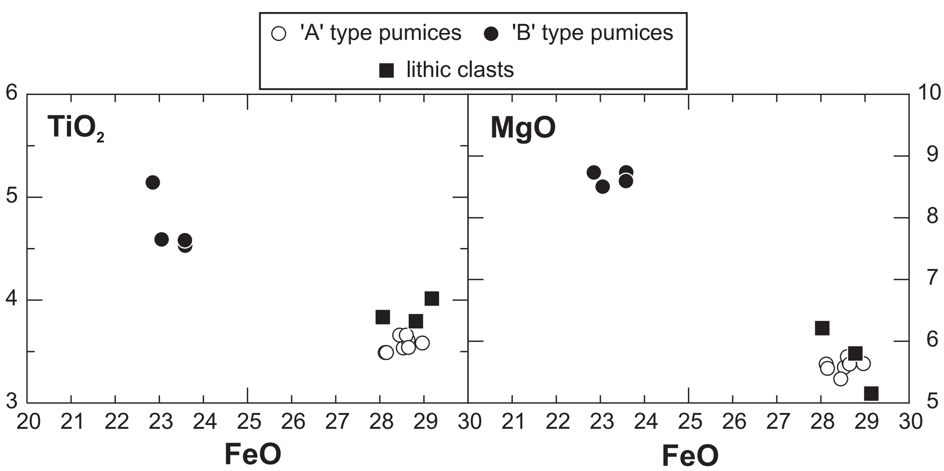

Fig. 7
Biotite composition in FeO vs. TiO2 and FeO vs. MgO diagrams. Biotite from the two types of pumice is clearly distinguished

Table 4
Representative biotite composition of the Harsány ignimbrite

Locality	Tiboldaróc				Harsány						
Type	'B'-type pumice				'A'-type pumice						
Sample	n9bi1	n9bi2	n9bi3	n9bi6	n20-2bi1	n20-2bi2	n20bi1	n20bbi2	N20b bi3	H5-1bi2	H5-1bi4
SiO_2	35.01	35.50	35.89	35.29	34.17	34.27	34.49	34.43	34.52	34.66	34.53
TiO_2	5.14	4.53	4.59	4.58	3.58	3.54	3.61	3.66	3.54	3.78	3.82
Al_2O_3	13.34	13.51	13.22	13.50	13.37	13.25	13.23	13.46	13.69	12.78	13.02
FeO	22.85	23.59	23.05	23.58	28.97	28.53	28.64	28.60	28.65	28.80	28.05
MnO	0.18	0.17	0.12	0.17	0.40	0.40	0.38	0.40	0.37	0.37	0.38
MgO	8.74	8.74	8.50	8.59	5.64	5.58	5.65	5.75	5.63	5.79	6.20
Na_2O	0.53	0.55	0.46	0.45	0.51	0.45	0.51	0.45	0.47	0.43	0.36
K_2O	8.28	8.34	8.29	8.27	8.36	8.37	8.56	8.71	8.50	8.56	8.59
Total	94.12	94.99	94.14	94.46	95.00	94.39	95.07	95.47	95.39	95.17	94.96

Discussion

Model 1: accidental lithic origin

The Harsány ignimbrite contains pumice blocks and coarse lapilli, which show a bimodal composition. The bimodality is also reflected by the composition of biotite. A possible explanation for the occurrence of the heterogeneous pumice population is that, following the plinian eruption of the 'A'-type rhyolitic magma, the laterally spreading pyroclastic flow picked up fragments from the surface covered by an older ignimbrite deposit. Indeed there were repeated eruptions of silicic magma during the Miocene, as indicated by the several ignimbrite units in the BVF. However, we have not found any ignimbrite unit with pumice of similar bulk rock and mineral composition akin to the 'B'-type pumice. In addition we would expect a more thorough incorporation of the older ignimbrite material, which we did not observe. Furthermore, it appears that the 'B'-type pumice is well distributed in the Harsány ignimbrite, since it can be found in equal amounts in localities separated from each other by the distance of about 10 km. Thus, the accidental lithic origin of the 'B'-type pumice can be excluded.

Model 2: stratified magma chamber

Compositionally heterogeneous rhyolite ignimbrite could be derived from a chemically stratified magma chamber, where the distinct zones are linked via fractional crystallization (Hildreth 1981, 2004; Brown et al. 1998). Although the two pumice types have fairly similar SiO_2 content, they show distinct trace element compositions. In a highly silicic magma system, concentration of trace elements is strongly controlled by the crystallization of accessory minerals such as ilmenite, zircon and allanite. The 'B'-type pumice typically has a higher light rare earth element (LREE), but lower heavy rare earth element (HREE) content, compared with the 'A'-type pumice. In addition the 'B'-type pumice shows less degree of a negative Eu-anomaly. This difference cannot be explained by crystallization of zircon, which has high distribution coefficients for HREE and very low ones for the LREE (Mahood and Hildreth 1983; Thomas et al. 2002; Sano et al. 2002; Lukács et al. 2005). Thus, crystallization of a small amount of zircon would decrease significantly the HREE, but would result in only a small change in the LREE. Ilmenite crystallization would have the same effect, but to a smaller degree. Additionally, ilmenite fractionation would also decrease the Nb concentration, which we cannot see in any of the two pumice types. Thus the trace element compositional difference between the two pumice types cannot be explained by zircon and/or ilmenite crystallization. The characteristic difference in LREE between the two pumice types can be resolved, however, by crystallization of allanite. This mineral occurs in the Harsány ignimbrite in small amounts. Allanite strongly incorporates the rare earth elements, particularly LREE (Mahood and Hildreth 1983). Considering only 0.03% allanite crystallization from the 'B'-type rhyolitic magma, we would obtain exactly the LREE distribution of the 'A'-type rhyolite (Fig. 8A). However, this influences neither the HREE content nor the Eu concentration. In order to achieve the 'A'-type pumice heavy rare earth element composition from the 'B'-type rhyolite, crystallization of 25–30% plagioclase and/or K-feldspar must be taken into account (Fig. 8B). Therefore, combining a very small amount of allanite and moderate feldspar crystallization, the trace element composition of 'A'-type pumice can be effectively modeled, assuming 25% fractionated minerals (Fig. 8C). This significant amount of mineral separation should, however, also be reflected in the major element composition, which we cannot observe (Fig. 8D). Therefore, a single stratified magma chamber model with discrete silicic melt zones and different degrees of differentiation can be excluded as a possible

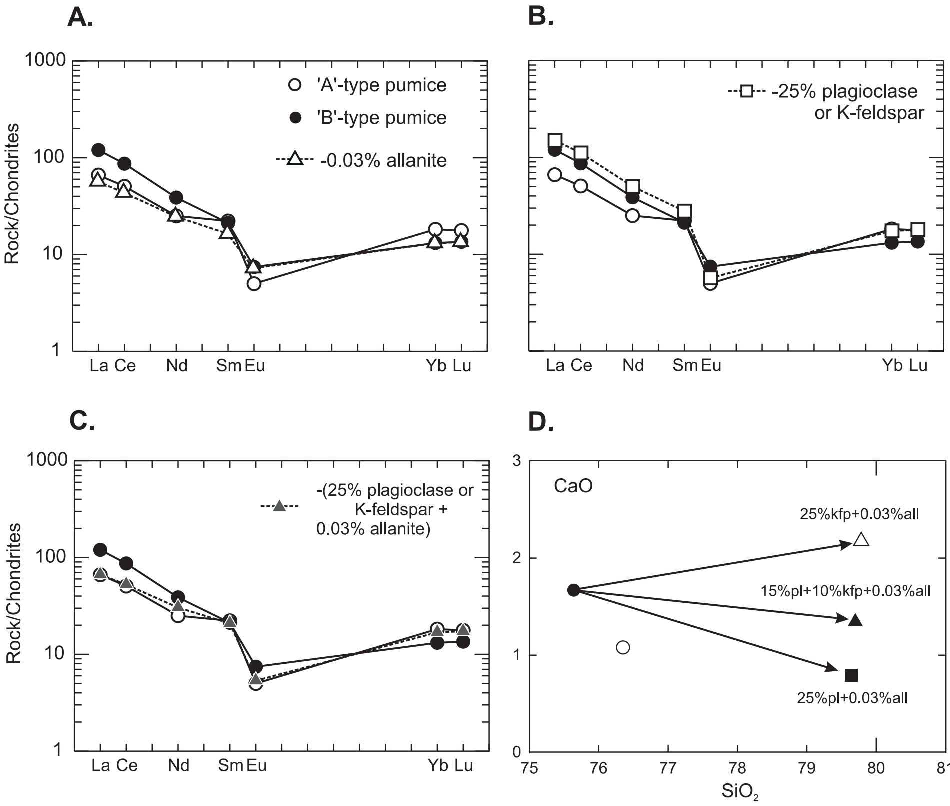

Fig. 8
Rare earth element modeling for the effect of crystallization of allanite (A) and plagioclase or K-feldspar (B) and both minerals (C) assuming 'B'-type pumice composition of the parental magma. Although crystallization of 0.03% allanite (all) and 25% plagioclase (pl) or K-feldspar (kfp) could result in the composition of the 'A'-type pumice, this would also significantly change the major element composition, which we cannot observe (D). Allanite and feldspar distribution coefficients after Mahood and Hildreth (1983). Chondrite data after Sun and McDonough (1989)

explanation for the heterogeneous pumice composition of the Harsány ignimbrite.

Model 3: derivation from isolated magma batches and syn-eruptive magma mingling

The bimodal geochemical character of the pumices in the Harsány ignimbrite could reflect rhyolitic magma batches derived from spatially separated magma chambers in the crustal reservoir (Fig. 9A). Slightly different magmatic evolution could have taken place in the magma chambers. Variations in the CaO, Sr and Eu concentrations of the pumice and glass (Figs 4 and 5) suggest that less plagioclase fractionation led to the formation of the 'B'-type rhyolitic melt compared with the 'A'-type magma. In the 'B'-type rhyolitic magma more magnesian biotite (Fig. 7) was crystallized. Another notable difference between the two pumice types is found in their trace element contents. Much of the trace element abundances in high-Si melts are primarily governed by the separation of accessory minerals. Different amounts of allanite and zircon separation could explain the trace element variations between the two rhyolite types.

Estimation of intensive parameters, such as temperature, pressure and oxygen fugacity, could help in the reconstruction of the relative position and condition of the isolated 'A'-type and 'B'-type rhyolitic magma storage zones. Unfortunately, the lack of appropriate mineral phases (e.g. Ti-magnetite and ilmenite pairs or plagioclase-hornblende pairs) does not enable estimating the intensive parameters for the rhyolitic magma. Crystallization closure pressure, at which quartz and plagioclase crystallized in equilibrium with the matrix glass, can be calculated by projecting the glass compositions onto the Qz-Ab-Or-H_2O system, using the method of Blundy and Cashman (2001). This results in a closure pressure usually less than 50 MPa; only a few samples fall between the 50 MPa and 100 MPa lines. The large scatter and the unrealistic shallow depth result could be due to the slight peraluminous character of the Harsány glass, as indicated by the normative corundum content (c>1 wt%). Since the effect of normative corundum is not considered in the calculation scheme, the pressure estimation result might be spurious (Blundy and Cashman 2008). Nevertheless, these data imply that the two magma chambers could have been at roughly similar depths. The crystal-poor nature of both pumice types indicates that two residual, strongly differentiated melts could be involved in the explosive eruption. Such rhyolitic melts are usually accumulated at the roof zone of an extensive crystal mush region.

There is a growing number of examples indicating that a complex magma reservoir network can develop beneath active volcanoes, where magma resides in completely or partially isolated magma chambers (e.g. Nakamura 1995; Civetta et al. 1997; Signorelli et al. 1999; Smith et al. 2004; Shane et al. 2005, 2007, 2008; Pabst et al. 2007). Since the definition of the magma chamber is ambiguous in the literature (e.g. Hildreth and Wilson 2007; Bachmann and Bergantz 2008), it is

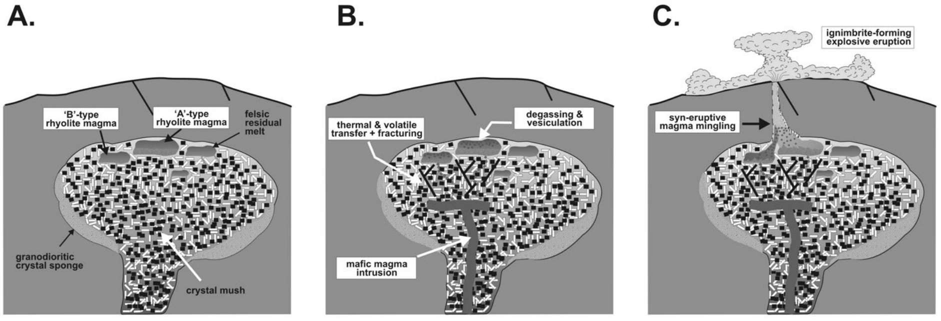

Fig. 9
Conceptual model for the processes in the magma reservoir led to the eruption of the Harsány ignimbrite. A. Formation of spatially separated rhyolitic melt lenses (magma chambers) at the roof zone of the extended crystal mush body (magma reservoir). In these melt pods slightly different crystallization processes could have taken place B. Intrusion of hot mafic magma resulted in heat-flux and volatile transfer as well as fracturing of the semi-rigid crystal mush. As a consequence degassing and vesiculation commenced in the rhyolitic magma chambers. C. Contemporaneous foaming and withdrawal of two rhyolitic magmas resulted in syn-eruptive mingling and violent ignimbrite-forming eruption

necessary to indicate how we use this term. We define the magma chamber here as a storage zone, where eruptible magma with much less than 50% crystal fraction is accumulated (it is also called melt lens by Hildreth and Wilson 2007, and melt pod by Shane et al. 2008), whereas magma reservoirs are much larger and include a huge fraction of crystal mush, which is usually uneruptible due to its high viscosity. At the roof zone of the porous crystal mush system, high-Si rhyolitic melts, having undergone different crystallization processes and cooling histories, could be formed in spatially isolated magma chambers. The final dominant crystallization of quartz and feldspar (plagioclase and/or K-feldspar) leads to water-saturated interstitial melts with fairly similar major element composition. However, crystallization of accessory minerals can result in different trace element signatures. The composition of the two pumice types in the Harsány ignimbrite is consistent with such a situation. The volume of the erupted rhyolitic magma depends on the extent of the silicic magma chamber. A large volume-rhyolitic eruption such as that of the Bishop tuff (about 600 km^3 in volume) requires amalgamation of the separated small magma chambers (Hildreth 2004; Hildreth and Wilson 2007). In other cases the spatially separated liquid pods are coevally withdrawn, as happened during the Glass Mountain eruptions in the pre-caldera stage of the Long Valley volcanism (Hildreth and Wilson 2007) and during the Okareka eruption of the Tarawera volcanic complex in the Taupo zone (Shane et al. 2008). In the latter case the erupted product involved fragments of at least three distinct rhyolitic bodies. The exact volume of the Harsány ignimbrite is hard to estimate due to incomplete exposure and the lack of knowledge about the source region. However, it should have been much less than those produced by the large volume (>100 km^3 in volume) silicic eruptions and is comparable with the small to intermediate size eruptions of the Taupo volcanic zone. This situation could favor the formation of spatially separated magma chambers within the magma reservoir rather than formation of a single big one.

The triggering mechanism of the violent volcanic eruption is often intrusion of basaltic magma into the more evolved felsic magma chamber (Sparks et al. 1977; Pallister et al. 1996; Murphy et al. 2000; Nairn et al. 2004), but in some cases the arrival of a new rhyolitic magma reactivates another rhyolite magma at depth (Eichelberger et al. 2000; Eichelberger and Izbekov 2000; Smith et al. 2004; Shane et al. 2008). In the Harsány eruption episode, no sign of basaltic intrusion can be observed. However, the role of a mafic magma cannot be excluded in the form of providing thermal and volatile transfer and crustal fracturing in the magma reservoir (Fig. 9B). As a result, the ponded, separated rhyolitic melts could come in contact with each other; the coeval decompression-induced degassing would lead to simultaneous foaming and, as a consequence, to a violent explosive eruption (Fig. 9C). The relative volume ratio between the two magma types cannot be determined precisely, since distinction between the two pumice types is impossible in the field. They can only be differentiated by detailed geochemical investigation. Among the collected and analyzed pumice clasts we have found mostly 'A'-type pumice. In addition, the host ignimbrite also has a dominant 'A'-type character, as reflected by the composition of glass shards and biotite. Based on these observations a conservative estimate of the relative volume ratio between the 'A'-type and 'B'-type magma could be about 80:20. Thus, the 'A'-type rhyolite magma was the dominant erupted magma. The lack of intermingled pumice and mixed mineral phases indicate no pre-eruptive mixing of these magma types. Thus they could come in contact with each other just prior to or during the eruption, and mixed incompletely in the course of rapid ascent to the surface.

In conclusion, the Harsány ignimbrite provides an example for syn-eruptive mingling of rhyolitic magma types. The distinct pumices, which represent isolated rhyolitic magma batches, can only be recognized by detailed geochemical work. This emphasizes the importance of thorough geochemical investigations in the petrogenetic and correlation studies of ignimbrite units.

Acknowledgements

This work was partially supported by the Marie Curie Training Site of the Institute of Mineralogy and Crystallography, University of Vienna, for the principal author. The fieldwork was financially supported by the Pro Renovanda Culturae Foundation (DT.2001.nov./21). The analytical work was carried out under the support of the Austrian–Hungarian Exchange Program (TET) at the Institute of Lithospheric Studies, University of Vienna. Trace element analysis of the glass shards were carried during a NATO fellowship for the second author in Utrecht. The authors thank P. Nagl, F. Koller, M. Balla, and K. Lengauer for their help during the geochemical analyses and to A. Beran and E. Libowitzky for supporting the principal author during her stay in Vienna at the Marie Curie Training Site. Ioan Seghedi and Teréz Póka are thanked for the constructive remarks on the manuscript.

References

Abdel-Rahman, A.-F.M. 1994: Nature of biotites from alkaline, calc-alkaline, and peraluminous magmas. – Journal of Petrology, 35, pp. 525–541.

Bachmann, O., G.W. Bergantz 2004: On the origin of crystal-poor rhyolites: extracted from batholithic crystal mushes. – Journal of Petrology, 45, pp. 1565–1582.

Bachmann, O., G.W. Bergantz 2008: The magma reservoirs that feed supereruptions. – Elements, 4, pp. 17–21.

Bachmann, O., M.A. Dungan, P.W. Lipman 2002: The Fish Canyon magma body, San Juan volcanic field, Colorado: rejuvenation and eruption of an upper-crustal batholith. – Journal of Petrology, 43, pp. 1469–1503.

Bachmann, O., C.F. Miller, S.L. de Silva 2007: The volcanic-plutonic connection as a stage for understanding crustal magmatism. – Journal of Volcanology and Geothermal Research, 167, pp. 1–23.

Blundy, J., K. Cashman 2001: Ascent-driven crystallisation of dacite magmas at Mount St Helens 1980–1986. – Contributions to Mineralogy and Petrology, 140, pp. 631–650.

Blundy, J., K. Cashman 2008: Petrologic reconstruction of magmatic system variables and processes. – Reviews in Mineralogy and Geochemistry, 69, pp. 179–239.

Brown, S.J.A., C.J.N. Wilson, J.W. Cole, J. Wooden 1998: The Whakamaru group ignimbrites, Taupo Volcanic Zone, New Zealand: evidence for reverse tapping of a zoned silicic magmatic system. – Journal of Volcanology and Geothermal Research, 84, pp. 1–37.

Capaccioni, B., N. Coradossi, R. Harangi, Sz. Harangi, D. Karátson, D. Sarocchi, L. Valentini 1995: Early Miocene pyroclastic rocks of the Bükkalja Ignimbrite Field (North Hungary) – A preliminary stratigraphic report. – Acta Vulcanologica, 7/2, pp. 119–124.

Civetta, L., G. Orsi, L. Pappalardo, R.V. Fisher, G. Heiken, M. Ort 1997: Geochemical zoning, mingling, eruptive dynamics and depositional processes – the Campanian Ignimbrite, Campi Flegrei caldera, Italy. – Journal of Volcanology and Geothermal Research, 75, pp. 183–219.

Czuppon, G., S. Harangi, T. Ntaflos, R. Lukács, C. Szabó, F. Koller 2001: Mixed andesite-rhyolite ignimbrite from the Miocene Bükkalja Ignimbrite Volcanic Field, Northern Hungary: evidence for magma mixing. – Mitteilungen der Österreichischen Mineralogischen Gesellschaft, 146, pp. 61–63.

DeCorte, F. 1987: The ko – standardization method – a move to optimisation of NAA. – Ph.D. Thesis. University of Gent.

Devine, J.D., J.E. Gardner, H.P. Brack, G.D. Layne, M.J. Rutherford 1995: Comparison of analytical methods for estimating H2O contents of silicic volcanic glasses. – American Mineralogist, 80, pp. 319–328.

Eichelberger, J.C., D.G. Chertkoff, S.T. Dreher, C.J. Nye 2000: Magmas in collision: Rethinking chemical zonation in silicic magmas. – Geology, 28, pp. 603–606.

Eichelberger, J.C., P.E. Izbekov 2000: Eruption of andesite triggered by dike injection: contrasting cases at Karymsky volcano, Kamchatka and Mount Katmai, Alaska. – Philosophical Transactions – Royal Society. Mathematical, Physical and Engineering Sciences, 358, pp. 1465–1485.

Harangi, S. 2001: Neogene to Quaternary Volcanism of the Carpathian–Pannonian Region – a review. – Acta Geologica Hungarica, 44, pp. 223–258.
Harangi, S., H. Downes, M. Thirlwall, K. Gmeling 2007: Geochemistry, petrogenesis and geodynamic relationships of Miocene calc-alkaline volcanic rocks in the Western Carpathian Arc, eastern central Europe. – Journal of Petrology, 48, pp. 2261–2287.
Harangi, S., L. Lenkey 2007: Genesis of the Neogene to Quaternary volcanism in the Carpathian–Pannonian Region: role of subduction, extension and mantle plume. – In: L. Beccaluva, G. Bianchini M. Wilson (Eds): Cenozoic volcanism in the Mediterranean area. Geological Society of America Special Paper 418, pp. 67–92.
Harangi, S., R. Lukács, G. Czuppon, C. Szabó 2002: Magma mixing in a compositionally layered magma chamber: a silicate melt inclusion study. In: B. Devivo, R.J. Bodnar (Eds): Workshop on Volcanic Systems, Seiano, Italy, pp. 101–106.
Harangi, S., P.R.D. Mason, R. Lukács 2005: Correlation and petrogenesis of silicic pyroclastic rocks in the Northern Pannonian Basin, Eastern–Central Europe: In situ trace element data of glass shards and mineral chemical constraints. – Journal of Volcanology and Geothermal Research, 143, pp. 237–257.
Hildreth, W. 1981: Gradients in silicic magma chambers: Implications for lithospheric magmatism. – J. Geophysical Research, 86, pp. 10153–10192.
Hildreth, W. 2004: Volcanological perspectives on Long Valley, Mammoth Mountain, and Mono Craters: several contiguous but discrete systems. – Journal of Volcanology and Geothermal Research, 136, pp. 169–198.
Hildreth, W., C.J. Wilson 2007: Compositional zoning of the Bishop tuff. – Journal of Petrology, 48, pp. 951–999.
Lexa, J., V. Konecný 1998. Geodynamic aspects of the Neogene to Quaternary volcanism. – In: Rakús, M. (Ed.): Geodynamic development of the Western Carpathians. Geological Survey of Slovak Republic, Bratislava, pp. 219–240.
Lowenstern, J.B. 1995: Applications of silicate melt inclusions to the study of magmatic volatiles. – In: Thompson, J.F.H. (Ed.): Magmas, Fluids and Ore Deposits. Mineralogical Association of Canada Short Course Volume 23, pp. 71–99.
Lukács, R., G. Czuppon, S. Harangi, C. Szabó, T. Ntaflos, F. Koller 2002: Silicate melt inclusions in ignimbrites, Bükkalja Volcanic Field, Northern Hungary – texture and geochemistry. – Acta Geologica Hungarica, 45, pp. 319–336.
Lukács, R., S. Harangi 2002: Petrogenesis of the Miocene silicic magmas in the Pannonian Basin: A case study in the Eastern Bükkalja Volcanic Field, Northern Hungary. – Geologica Carpathica, 53, pp. 13–14.
Lukács, R., S. Harangi, T. Ntaflos, F. Koller, Z. Pécskay 2007: A Bükkalján megjelenő felső riolittufaszint vizsgálati eredményei: a harsányi ignimbrit egység (The characteristics of the Upper Rhyolite Tuff Horizon in the Bükkalja Volcanic Field: The Harsány ignimbrite unit). – Földtani Közlöny, 137, pp. 487–514.
Lukács, R., S. Harangi, T. Ntaflos, P.R.D. Mason 2005: Silicate melt inclusions in the phenocrysts of the Szomolya Ignimbrite, Bükkalja Volcanic Field (Northern Hungary): implications for the magma chamber processes. – Chemical Geology, 223, pp. 46–67.
Lukács, R., S. Harangi, I. Oláh 2001: Correlation of Miocene pumice-bearing pyroclastic deposits in the Pannonian Basin. – Mitteilungen der Österreichischen Mineralogischen Gesellschaft, 146, pp. 180–182.
Lukács, R., Sz. Harangi, Gy. Radócz, M. Kádár, Z. Pécskay, T. Ntaflos 2010: The nature of the Miocene volcanic products of the boreholes Miskolc-7, Miskolc-8 and Nyékládháza-1 and their correlation with the ignimbrites of Bükkalja – Földtani Közlöny, 140 pp. 445–468. (In Hungarian with English abstract.)
Mahood, G., W. Hildreth 1983: Large partition coefficients for trace elements in high-silica rhyolites. – Geochimica et Cosmochimica Acta, 47, pp. 11–30.

Márton, E., L. Fodor 1995: Combination of palaeomagnetic and stress data – a case study from North Hungary. – Tectonophysics, 242, pp. 99–114.
Márton, E., Z. Pécskay 1998: Complex evaluation of paleomagnetic and K/Ar isotope data of the Miocene ignimbritic volcanics in the Bükk Foreland, Hungary. – Acta Geologica Hungarica, 41, pp. 467–476.
Márton, E., T. Zelenka, P. Márton 2007: Paleomagnetic correlation of Miocene pyroclastics of the Bükk Mts. and their forelands. – Central European Geology, 50/1, pp. 47–57.
Mason, P.R.D., W.J. Kraan 2002: Attenuation of spectral interferences during laser ablation inductively coupled plasma mass spectrometry (LA-ICP-MS) using an rf only collision and reaction cell. – Journal of Analytical Atomic Spectrometry, 17, pp. 858–867.
Murphy, M.D., R.S.J. Sparks, J. Barclay, M.R. Carroll, T.S. Brewer 2000: Remobilization of andesite magma by intrusion of mafic magma at the Soufriere Hills volcano, Montserrat, West Indies. – Journal of Petrology, 41, pp. 21–42.
Nairn, I.A., P.R. Shane, J.W. Cole, G.J. Leonard, S. Self, N. Pearson 2004: Rhyolite magma processes of the ~AD 1315 Kaharoa eruption episode, Tarawera volcano, New Zealand. – Journal of Volcanology and Geothermal Research, 131, pp. 265–294.
Nakamura, M. 1995: Continuous mixing of crystal mush and replenished magma in the ongoing Unzen eruption. – Geology, 23, pp. 807–810.
Pabst, S., G. Wörner, L. Civetta, R. Tesoro 2008: Magma chamber evolution prior to the Campanian Ignimbrite and Neapolitan Yellow Tuff eruptions (Campi Flegrei, Italy). – Bulletin of Volcanology, 70, pp. 961–976.
Pallister, J.S., R.P. Hoblitt, G.P. Meeker, R.J. Knight, D.F. Siems 1996: Magma mixing at Mount Pinatubo: petrographic and chemical evidence from the 1991 deposits. – In: Newhall, C.G., R.S. Punongbayan (Eds): Fire and Mud: Eruptions and Lahars of Mount Pinatubo, Philippines. Univ Wash Press, pp. 687–731.
Pantó, G. 1962: The role of ignimbrites in the volcanism of Hungary. – Acta Geologica Academiae Scientiarum Hungaricae, 6/3–4, 307 p.
Pécskay, Z., J. Lexa, A. Szakács, I. Seghedi, K. Balogh, V. Konecny, T. Zelenka, M. Kovacs, T. Póka, A. Fülöp, E. Márton, C. Panaiotu, V. Cvetkovic 2006: Geochronology of Neogene magmatism in the Carpathian arc and intra-Carpathian area. – Geologica Carpathica, 57, pp. 511–530.
Póka, T. 1988. Neogene and Quaternary volcanism of the Carpathian–Pannonian region: changes in chemical composition and its relationship to basin formation. – In: Royden, L.H., F. Horváth (Eds): The Pannonian Basin. A study in basin evolution. AAPG Memoirs, pp. 257–277.
Póka, T., T. Zelenka, A. Szakács, I. Seghedi, G. Nagy, A. Simonits 1998: Petrology and geochemistry of the Miocene acidic explosive volcanism of the Bükk Foreland; Pannonian Basin, Hungary. – Acta Geologica Hungarica, 41/4, pp. 399–428.
Sano, Y., K. Terada, T. Fukuoka 2002: High mass resolution ion microprobe analysis of rare earth elements in silicate glass, apatite and zircon: lack of matrix dependency. – Chemical Geology, 184, pp. 217–230.
Seghedi, I., H. Downes, O. Vaselli, A. Szakács, K. Balogh, Z. Pécskay 2004: Post-collisional Tertiary–Quaternary mafic alkalic magmatism in the Carpathian–Pannonian region: a review. – Tectonophysics, 393, pp. 43–62.
Shane, P., S.B. Martin, V.C. Smith, K.F. Beggs, M.B. Darragh, J.W. Cole, I.A. Nairn 2007: Multiple rhyolite magmas and basalt injection in the 17.7 ka Rerewhakaaitu eruption episode from Tarawera volcanic complex, New Zealand. – Journal of Volcanology and Geothermal Research, 164, pp. 1–26.
Shane, P., I.A. Nairn, V.C. Smith 2005: Magma mingling in the ~50 ka Rotoiti eruption from Okataina Volcanic Centre: implications for geochemical diversity and chronology of large volume rhyolites. – Journal of Volcanology and Geothermal Research, 139, pp. 295–313.
Shane, P., I.A. Nairn, V.C. Smith, M. Darragh, K. Beggs, J.W. Cole 2008: Silicic recharge of multiple rhyolite magmas by basaltic intrusion during the 22.6 ka Okareka Eruption Episode, New Zealand. – Lithos, 103, pp. 527–549.

Signorelli, S., G. Vaggelli, L. Francalanci, M. Rosi 1999: Origin of magmas feeding the Plinian phase of the Campanian Ignimbrite eruption, Phlegrean Fields (Italy): constraints based on matrix-glass and glass-inclusion compositions. – Journal of Volcanology and Geothermal Research, 91, pp. 199–220.
Smith, V.C., P. Shane, I.A. Nairn 2004: Reactivation of a rhyolitic magma body by new rhyolitic intrusion before the 15.8 ka Rotorua eruptive episode: implications for magma storage in the Okataina Volcanic Centre, New Zealand. – Journal of the Geological Society, 161, pp. 757–772.
Sparks, S.R.J., H. Sigurdsson, L. Wilson 1977: Magma mixing: a mechanism for triggering acid explosive eruptions. – Nature, 267, pp. 315–318.
Sun, S. S., W.F. McDonough 1989: Chemical and isotopic systematics of oceanic basalts: implications for mantle composition and processes. – In: Saunders, A.D., M.J. Norry (Eds): Magmatism in the oceanic basins. Geol. Soc. Spec. Publ. No. 42, pp. 313 345.
Szabó, C., S. Harangi, L. Csontos 1992: Review of Neogene and Quaternary volcanism of the Carpathian–Pannonian region. – Tectonophysics, 208, pp. 243–256.
Szabó, Z. 2000: Cirkonmorfológiai vizsgálatok a Bükkalja miocén piroklasztit sorozatain (A zircon morphology study on the Miocene silicic pyroclastic rocks of the Bükkalja). – Szakdolgozat. ELTE Kőzettan–Geokémiai Tanszék, 111 p.
Szabó, Z., S. Harangi 2001: A zircon morphology study on the Miocene silicic pyroclastic rocks of the Bükkalja Volcanic Field, Northern Hungary. – PANCARDI 2001, Abstract Volume, p. 12.
Szakács, A., T. Zelenka, E. Márton, Z. Pécskay, T. Póka, I. Seghedi 1998: Miocene acidic explosive volcanism in the Bükk Foreland, Hungary: Identifying eruptive sequences and searching for source locations. – Acta Geologica Hungarica, 41, pp. 413–435.
Thomas, J.B., R.J. Bodnar, N. Shimizu, A.K. Sinha 2002: Determination of zircon/melt trace element partition coefficients from SIMS analysis of melt inclusions in zircon. – Geochimica et Cosmochimica Acta, 66, pp. 2887–2901.
Walsh, J.N., F. Buckley, J. Barker 1981: The simultaneous determination of the rare-earth elements in rocks using inductively coupled plasma source spectrometry. – Chemical Geology, 33, pp. 141–153.
Wark, D.A., W. Hildreth, F.S. Spear, D.J. Cherniak, E.B. Watson 2007: Pre-eruption recharge of the Bishop magma system. – Geology, 35, pp. 235–238.
Wilson, C.J.N., S. Blake, B.L.A. Charlier, A.N. Sutton 2006: The 26.5 ka Oruanui eruption, Taupo volcano, New Zealand: development, characteristics and evacuation of a large rhyolitic magma body. – Journal of Petrology, 47, pp. 35–69.